Particulate Two-Phase Flow

Edited by

M.C. Roco

National Science Foundation and
University of Kentucky

With 50 contributing authors

Butterworth–Heinemann

Boston London Oxford Singapore Sydney Toronto Wellington

CHAPTER 10

FINITE SIZE EFFECTS IN FLUIDIZED SUSPENSION EXPERIMENTS

D. Joseph

10.1 INTRODUCTION

"Two fluid" equations for fluidized suspensions of solid particles can be rigorously formulated as ensemble averages (Joseph and Lundgren 1990). Even though these equations have a rigorous foundation they are not useful unless the interaction forces are correctly modeled. Modeling, the framing of constitutive hypotheses, is basically a guess about the solutions of the equations of motion. A constitutive hypothesis is when you guess what the solution of a problem of dynamics might be without actually obtaining the solution.

Conventional theories of fluidized suspensions are generally formulated as one-dimensional approximations in which quantities perpendicular to the direction of flow are averaged over cross sections. One-dimensional theories describe the evolution in time t of averaged quantities in the direction z of flow. A one-dimensional, two-phase flow (Wallis 1969) is a system of four "two-fluid" equations for the volume fraction α of solids, the volume fraction $\varepsilon = 1 - \alpha$ of fluids, the average particle velocity $u_p = u$ and fluid velocity u_f. In one-dimensional, one-phase flows (Foscolo and Gibilaro 1984, 1987; Batchelor 1988, Joseph 1990) the forces which the fluid exert on the solids are modeled, and the decoupled equations for α and u are of interest. The modeling of forces in two-phase and one-phase flows is fraught with difficulties. It is not even clear what the variables should be as our discussion in §10.3 of finite size effects will reveal. In one-phase theories it is not even possible to guarantee that the range $\alpha\,(z,t) \in [0,1]$ will be protected (Singh and Joseph 1990). Moreover, there are three effects of fundamental importance which are omitted entirely in conventional one-dimensional theories: finite size effects §10.3); wakes §10.4); and turning couples on long bodies leading to stable fluidized structures which we call wake architectures §10.5). In this essay we shall focus our attention on these omitted finite size and nonlinear effects.

10.2 ONE-DIMENSIONAL, ONE-PHASE FLOW

Conventional theories are framed in terms of conservation equations for the number density $N = \rho\alpha/m$ of particles of mass m and density ρ whose mass centers are on the plane z. Since ρ and m are constant,

$$\alpha_t + (\alpha\, u)_x = 0. \qquad (10.2.1)$$

The momentum equation of motion may be written in the first order approximation as

$$\rho\alpha\,(U_t + uu_z) = \mathfrak{F}[\alpha,u] - \Pi_z\,[\alpha,u] \qquad (10.2.2)$$

where $\Pi\,[\alpha,u]$ is the particle phase pressure, (10.2.1) and (10.2.2) are the equations for the particle phase and

$$\Pi_z = \Pi_\alpha\,\alpha_z + \Pi_u\,U_z\,. \qquad (10.2.3)$$

Various kinds of modeling assumptions about $\mathfrak{F}$ and Π have been made by the authors named in §10.1. There are two points of view, Joseph (1990) argues that in a first order system of equations for α and u, one ought to assume say that Π_u and Π_α are not zero, unless an argument which says one or both are zero is given. In the other view, adopted by Batchelor (1988), it is necessary to give the reasons why Π_α or Π_u is not zero, from the point of view of physics, and he reasons that $\Pi_\alpha \neq 0$ but presents no argument to justify putting $\Pi_u = 0$. Foscolo and Gibilaro (1987) also try to obtain Π from a physical argument and they also get a Π that doesn't depend on u. Joseph (1990) noticed that you could write their Π_z as $\frac{2}{3}\,D\,\mathfrak{F}_\alpha\alpha_z$ with their $\mathfrak{F} = NF\,(\alpha,u)$ where N is the number density, D is the particle diameter and

$$F(u,\alpha) = m\tilde{g}\left\{-(1-\alpha) + \left[\frac{u_c-u}{U(0)}\right]^{\frac{4.8}{n}}(1-\alpha)^{-3.8}\right\} \qquad (10.2.4)$$

on a single particle. Here m is the mass of a single sphere of radius R, $\tilde{g} = (\rho - \rho_f)g/\rho$ is reduced gravity, ρ is the density of the sphere, ρ_f is the density of the fluid, $U(\alpha)$ is the steady fall velocity under gravity of a sphere in a uniform dispersion of spheres of solids fraction α. In a uniform dispersion $u = 0$ and α is independent of z. The fluidization velocity $u_c = u_f(1-\alpha) - u\alpha$, where u_f is the fluid velocity, is in general solenoidal, independent of z, and when $u = 0$, u_c satisfies the Richardson and Zaki correlation

$$u_c = U(\alpha) = U(0)\,(1-\alpha)^n\,. \qquad (10.2.5)$$

U(0) is the velocity of one sphere in a pure liquid and it can be expressed in terms of the Reynolds number using various empirical correlations and n(Re)

is the Richardson and Zaki exponent; it lies between 4.8 for small Reynolds numbers $Re = \frac{u_c 2R}{\nu}$ and 2.4 for large Re. The ingenious force law (10.2.4) was invented by Foscolo and Gibilaro but it cannot be regarded as established. Their argument about the form of Π_z does not exclude the idea that $\Pi = N_A F$ where $N_A = 4\alpha/\pi D^2$ is the number density per unit area, and $N_A/N = \frac{2}{3} D$. Then

$$\Pi_z = \tfrac{2}{3} D \, (\mathfrak{F}_\alpha \alpha_z + \mathfrak{F}_u U_z) \tag{10.2.6}$$

where $\mathfrak{F}_u \neq 0$.

In the early days it was thought that zeroth order approximation in which Π_z and higher derivatives are zero might suffice. In fact, zeroth order theories have been discredited partly because they give rise to Hadamard instability of the state of uniform fluidization.

The state of uniform fluidization, u=0 and $\alpha = \alpha_o$ where α_o is a constant, is a solution of (10.2.1) and (10.2.2) because $\mathfrak{F}[\alpha_o, 0] = 0$ (see §10.5) and $\Pi_z = 0$. To study stability we write $\alpha = \alpha_o + \psi$ linearize for small ψ and u where ψ and u satisfy

$$\psi_t + \alpha_o u_z = 0, \tag{10.2.7}$$

$$u_t = \hat{a} u - \hat{b} \psi - \hat{c} \psi_z - \hat{d} u_z. \tag{10.2.8}$$

The values

$$[\hat{a}, \hat{b}, \hat{c}, \hat{d}] =$$

$$\left[\frac{4.8 g}{n U(0)} (1 - \alpha_o)^n, \, 4.8 g, \, -\tfrac{2}{3} D \hat{b}, \, -\tfrac{2}{3} D \hat{a} \right] \tag{10.2.9}$$

used by Foscolo and Gibilaro (1987) with $\hat{d} = 0$ and by Joseph (1990) with $\hat{d} \neq 0$ are representative for all the conventional theories so far proposed. The dispersion relation

$$\sigma^2 + \sigma (\hat{a} - i\beta \hat{d}) + \alpha_o (\beta^2 \hat{c} + i\beta \hat{b}) = 0 \tag{10.2.10}$$

governs the growth rate σ to waves of length $2\pi/\beta$ of disturbance proportional to $\exp(\sigma t + i\beta x)$. When the particle phase pressure gradient $\Pi_z = 0$ so that $\hat{c} = \hat{d} = 0$, we get

$$\text{re}\,\sigma \to \sqrt{\hat{b}\alpha_o}\,\sqrt{\beta} \tag{10.2.11}$$

for large β. This is a catastrophic instability with an unbounded growth rate for small waves, a Hadamard instability with square root growth. The particle phase pressure will regularize this catastrophic instability, but the system with coefficients (10.2.6) is unstable with positive growth rates re σ (β) uniformly bounded in β, not Hadamard unstable. On the other hand, if $\hat{d} = 0$ but the other coefficients are as in (10.2.6), Foscolo and Gibilaro (1984, 1987) have shown that stability is possible and the criterion for instability is in good agreement with the formation of bubbling gas beds for some beds.

The considerations of the previous paragraph explain why so much attention has been given to the particle phase pressure in conventional theories of fluidized suspensions. Batchelor (1988) argues that the α_z term represents fluctuation induced diffusion against a gradient in which particles drift into empty places by random walks as in Brownian motions. The fluctuations here would have to be supplied by hydrodynamics, vortex shedding, unsteady particle motions or other causes whose magnitude areas are yet unknown.

Hadamard instabilities can also be regularized by higher order gradients; for example, by viscosity which is associated with a second derivative of u. Viscosity, like other gradient regularizers, will kill the short waves but will not stabilize an otherwise unstable system. The regularization of Hadamard instability is only one property among many which could be expected of a physically realistic mathematical theory. In the two-dimensional beds of large spherical particles studied by Singh and Joseph (1991a,b) there is a structured response in which certain discrete waves do not grow. These blocked wave lengths cannot be predicted from conventional gradient theories, but they are predicted by a global theory which accounts for the fact that the portion of the plane at z blocked by particles is determined also by spheres whose centers are not at z.

10.3 FINITE SIZE EFFECTS (Singh and Joseph 1990,1991a,b)

To account for the finite size of spheres we are going to introduce a third variable, the fractional area α^a, which is related to the volume fraction α by a convolution generated by the following construction. Consider a plane at z. Locate the origin of a coordinate x on z. Spheres at a distance $|x| < R$ from z intersect z and their area of intersection is $\pi(R^2 - x^2)$. If N(x+z,t) is the number density of spheres with centers at x+z, then N(x+z,t)Adx is the number of such spheres in an infinitesimal volume Adx, where A is the area of, say, some square $A = L^2$ with a very large L. The area A_s on the plane which is cut out by spheres is obtained by summing all of the areas of intersections coming from infinitesimal volumes centered on x+z as x varies from -R to R,

$$A_s = \int_{-R}^{R} N(x+z,t)\, \pi(R^2 - x^2)\, A\, dx. \qquad (10.3.1)$$

After writing $A_s/A = \alpha^a$, using $N = \rho\alpha/m = 3\alpha/4\pi R^3$, we get

$$\alpha^a = \frac{3}{4R^3} \int_{-R}^{R} \alpha(x+z,t)\, (R^2 - x^2)\, dx\ . \qquad (10.3.2)$$

When α is independent of x, then $\alpha^a(z,t) = \alpha(z,t)$. Since α is independent of x when R is small, our theory reduces, but not uniformly (see (10.3.12)), to the conventional one for small particles. The criterion for smallness is that the variation in number density of an ensemble average is small relative to the size of a particle.

10.3.1 Three-Variable Theory

We construct a three-variable theory by replacing the volume fraction in force law (10.2.4) and (10.2.5) with the area fraction α^a. A nonlinear three-variable theory without gradients is given by

$$\alpha_t + (u\alpha)_z = 0\,, \qquad (10.3.3)$$

$$\alpha^a = \frac{3}{4R^3} \int_{-R}^{R} \alpha(x+z,t)(R^2 - x^2)\, dx\,, \qquad (10.3.4)$$

$$u_t + uu_z = \tilde{g}\left\{-\varepsilon + \left[\frac{u_c - u}{U(0)}\right]^{\frac{4.8}{n}} e^{-3.8}\right\} \qquad (10.3.5)$$

where $\varepsilon = 1 - \alpha^a$ and the composite velocity u_c, which is the superficial velocity at the inlet of the bed is given in

$$u_c = U(0)\varepsilon_o^n. \qquad (10.3.6)$$

Uniform fluidization, $u = 0$ and $\alpha = \alpha_0$ is a solution of this system.

In our three-variable model we think of $\alpha(z,t)$ and $u(z,t)$ as an ensemble of averaged quantities. It is necessary to think of ensemble averages rather than volume averages because we shall be looking at fields with rapid variation over the length of the microstructure. The number density is then taken as $N = \rho/m\alpha$. The fractional area α^a is the convolution of an ensemble average and is not itself an ensemble average. In our experiments we actually measure α^a as simple averages over horizontal lines of pixels. The main idea of our model is to replace the volume fraction α with fractional area α^a in the force law, where α^a and α are related by the simple construction just given. We have constructed our model as a hypothesis which seems reasonable but which we cannot prove. We wish to draw out the predictions of our model and see how they compare with experiments. We should not be deterred by bogeyman mathematicians because we don't know the exact words to scare away the bogeyman.

10.3.2 Linearized Stability

Equations (10.3.3), (10.3.4) and (10.3.5) may be linearized around uniform fluidization; $\alpha = \alpha o + \psi$ where ψ is small. Then

$$\psi_t + \alpha_o u_z = 0,$$
$$\alpha_1^a = -\varepsilon_1 = \frac{3}{4R^3} \int_{-R}^{R} \psi(z+x,t)\, (R^2 - x^2)\, dx, \qquad (10.3.7)$$
$$u_t = \hat{a}u - \hat{b}\varepsilon_1$$

where $\hat{a}$, $\hat{b}$ are given by (10.2.6), and after eliminating ε_1 and u_1, we find

$$\psi_{tt} = -\hat{a}\,\psi_t - \hat{b}\frac{3\alpha_o}{4R^3}\frac{\partial}{\partial z} \int_{-R}^{R} \psi(z+x,t)\, (R^2 - x^2) dx\ . \qquad (10.3.8)$$

Writing $\psi = \psi_o\, e^{\sigma t}\, e^{i\beta z}$ we find a complex dispersion relation of the form

$$\sigma^2 + \sigma\hat{a} + i\beta\hat{b}\,\alpha_o\Theta(\beta R) = 0. \qquad (10.3.9)$$

where

$$\Theta(\beta R) = 3\left[\frac{\sin \beta R}{(\beta R)^3} - \frac{\cos \beta R}{(\beta R)^2}\right] \qquad (10.3.10)$$

is the blockage function (figure 10.3.1)

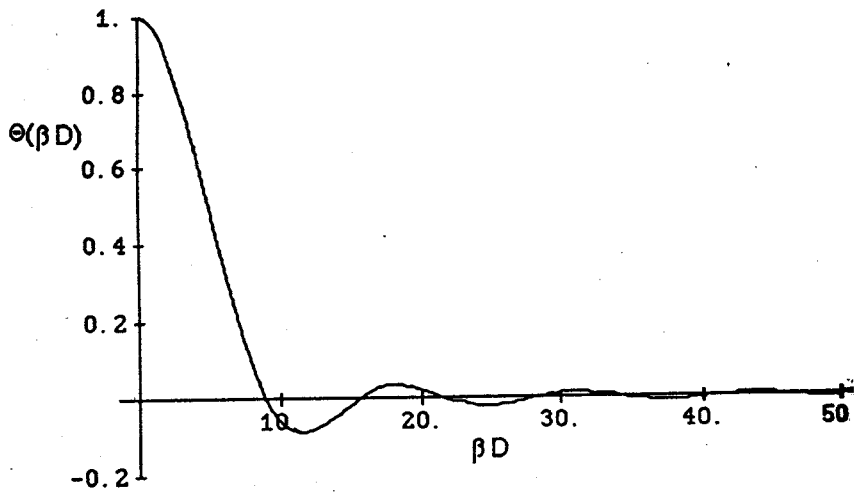

Figure 10.3.1 $\Theta(\beta D)$ is plotted as a function of (βD), D=2R.

We may solve the quadratic equation for

$$\sigma = -\frac{\hat{a}}{2} \pm \frac{\hat{a}}{2}\sqrt{1 - i\,\Sigma}, \qquad (10.3.11)$$

$$\Sigma = -\frac{4\beta\hat{\delta}\,\alpha_o\Theta(\beta R)}{\hat{a}^2}.$$

The most dangerous root is associated with the plus sign in (10.3.10) and with the first zero 2.6/D of $d(\beta\Theta/d\beta)$. At this most dangerous β,

$$\Sigma = \Sigma_m = \frac{2.17\, n^2\, \alpha_o u_c^2}{\varepsilon_o\, D\, \tilde{g}}. \qquad (10.3.12)$$

Singh and Joseph (1991a,b) have argued that Σ_m is a basic parameter distinguishing the response of different beds. The growth rate and frequency vanish, $\sigma = 0$, at the zeros of $\beta\Theta(\beta R)$, at $\beta = 0$, $\beta R = 4.493$, 7.7253, 10.904, etc., and $\beta\Theta(\beta R) \to 0$ for a fixed value of R, as $\beta \to \infty$. It follows that re $\sigma \to 0$ as $\beta \to \infty$ and our zeroth order model with blockage is always unstable but not Hadamard unstable. On the other hand, if β<1.3/R is large and fixed, then $\Theta(\beta R) \to 1$ as $R \to 0$ and our model reduces, nonuniformly, to the conventional one which is effectively but not actually Hadamard unstable. The value β= 1.3/R is a cutoff for Hadamard instability where the growth rate re σ is a maximum.

10.3.3 Nonlinear Theory (Singh and Joseph 1991b)

Singh and Joseph (1991b) solved the initial value problem for the three-variable, one-dimensional theory by numerical methods for periodic boundary and different initial conditions. No solutions of permanent form with discrete spectral peaks were found. Instead, they found chaotic solutions with nearly stationary levels of the power when a certain dimensionless "growth rate" parameter is below a critical value and unstable solutions whose power levels increase without bound when this value is above the critical one. The power spectrum of the bounded solutions is continuous and such that power levels are very low for wave numbers in the blocked set which are mariginally stable in the linear theory.

10.3.4 Comparison With Experiments

Singh and Joseph (1990) made video recordings of experiments on beds of fluidized spheres confined to move in two dimensions between glass plates. A typical configuration seen in the experiments look like the photograph shown in figure 10.3.2. Analysis of the digitized signals gives the fractional

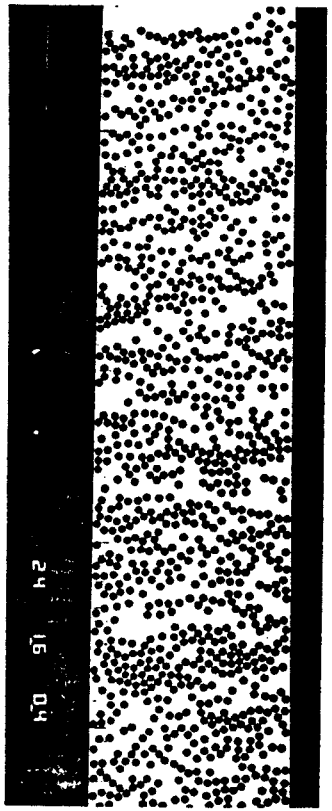

Figure 10.3.2 Fully expanded fluidized bed of plastic beads, Re=300, α=0.88. Most spheres line up in horizontal arrays, vertical pairs are drafting.

area as a function of space and time at a discrete set of points. The amplitude of the measured spectra is a strong function of frequency and wave number with deep minima at the blocked wave numbers predicted by stability theory and the numerical integration of the initial value problem. At low Reynolds numbers, the measured specturm looks like the growth rate function from linear theory. As the Reynolds number increases, the graph of the power spectrum gets higher energy at smaller wave numbers, consistent with the increasing importance of wake effects.

In figure 10.3.3 we have compared plots of the logarithm of the growth rate log (Reσ) from linear theory as a function of βD with the magnitude logα of the power spectrum from nonlinear theory and experiments. The blocked values of βD are evident in all cases. Many more and different comparisons of theory and experiments are discussed by Singh and Joseph (1990) with similar agreements. We think that the agreements between the predictions of the simple theory with finite size but no gradient are astonishing, since there are no disposable constants and nothing has been adjusted. On the other hand, the predictions of the gradient theory do not agree with the experiments on two-dimensional fluidizations of large particles. Using the Foscolo-Gibilaro theory with $\hat{d} = 0$ we find from (10.2.7) that the beds we used in our experiments are operating in regions of stable uniform fluidization with

Re=300, u_c=.044 m/s, α=0.8, n=3.0, D=0.0063 m, $\frac{\rho}{\rho_f}$=1.12, g=1.05 m/s^2.

It is difficult to use Batchelor's theory to check the stability since some of the coefficients are not known, but he says "...$\frac{\rho}{\rho_f}$ is seldom less than 2 for a marginally stable bed." These theories disagree with our experiments and those Volpicelli, Massimilla and Zenz (1966) in which all the flows were decidedly not uniform.

We have shown that finite size effects are effectively lost for sufficiently small particles where conventional theories with gradients may be appropriate. However, the Hadamard instability will never arise in the case of a small particle limit in the three-variable theory because the growth rate is a maximum at β=1.3/R, so that waves shorter than 2πR/1.3 are regularized. In the limiting theory β is not totally independent of R and a limit $\beta \to \infty$ for a fixed R is not useful.

10.4 WAKES AND TURNING COUPLES

It is not clear why the one-dimensional theory with finite size effects works so well. Perhaps one reason is that one-dimensional dynamics are generated by nonlinear effects associated with drafting, kissing and tumbling. This kind of one dimensional dynamics is evident in the photographs of two-dimensional beds shown in figure 10.3.2, which are like the ones studied by Singh and Joseph (1990) and in all the other photographs of two-dimensional fluidization shown in the papers of Volpicelli, et al. (1966), Fortes, Joseph and Lundgren (1987) and Joseph, Fortes, Lundgren and Singh (1987). It may not be a bad idea to base a force law for such a motion on a reliable empirical correlation, like the Richardson and Zaki (1954) correlations used

by Foscolo and Gibilaro in deriving (10.2.4) which is valid under the very nonlinear conditions prevailing in our experiments. It is perhaps appropriate here to note that Volpicelli, et al. (1966) showed that the Richardson-Zaki correlations do hold in two-dimensional beds of spheres after one accounts for the effects of walls in shifting the curves of correlation.

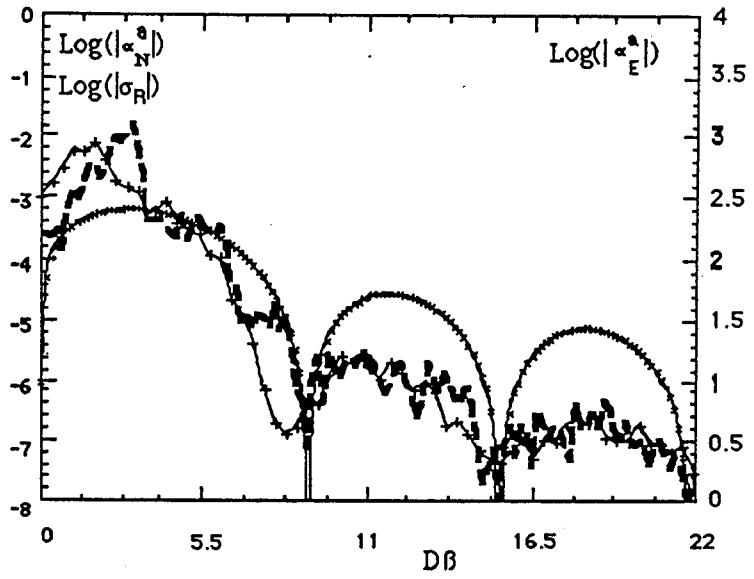

Figure 10.3.3 Comparison of log|σ_R| (——•——), log |α^a_N| (— — —) and log|α^a_E| (——+——), where σ_R is the real part of the growth rate of the linear theory of stability of uniform fluidization, log |α^a_N| is the amplitude of the power spectrum computed numerically for the three variable nonlinear theory and log|α^a_E| where α^a_E is the power spectrum measured in the experiments. The value of the parameter Σ_m which we estimated for the experiments is 1.79. For the nonlinear numerical solution Σ_m is 0.0958. The amplitude is a strong function of Σ_m, but the blocked wave numbers are robust, independent of sphere size or Reynolds number.

We may explain the dynamic generation of effective one-dimensional motions at modest, but not too small, Reynolds numbers larger than some critical value which may lie between 0.5 (Happel and Pfeffer 1960) and 8 (figure 10.4.2), as a pairwise coupling of spheres whose line of centers is parallel to the stream. We describe the dynamic scenario associated with this pairwise coupling as drafting, kissing and tumbling. The second sphere is drafted into the wake of the first sphere; they kiss, then tumble (figures 10.4.1, 10.4.2). The falling motion of kissing spheres whose line of centers is parallel to the stream is unstable to couples of the type which turn

streamlined bodies broadside on, stagnation point pressures of the type that cause an airship to stall (figure 10.4.3). Neighboring spheres with centers aligned cross stream are a characteristic feature easily observed in all photographs of two-dimensional fluidized beds (figures 10.3.2, 10.4.6, 10.4.7, 10.4.8, 10.5.1 and 10.5.2).

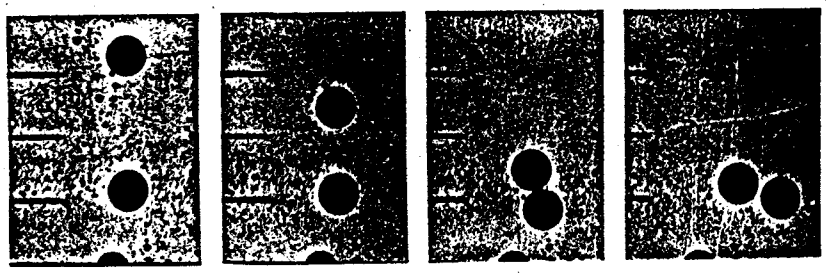

(a) (b) (c) (d)

Figure 10.4.1 Drafting, kissing of plastic spheres in water, Re=700: (a) the line of centers lies along the stream; (b) both spheres are falling but the second is falling faster than the first; (c) kissing after drafting; and (d) tumbling after kissing. Tumbling is an instability, well-known of long bodies which like to orient themselves broadside to the flow.

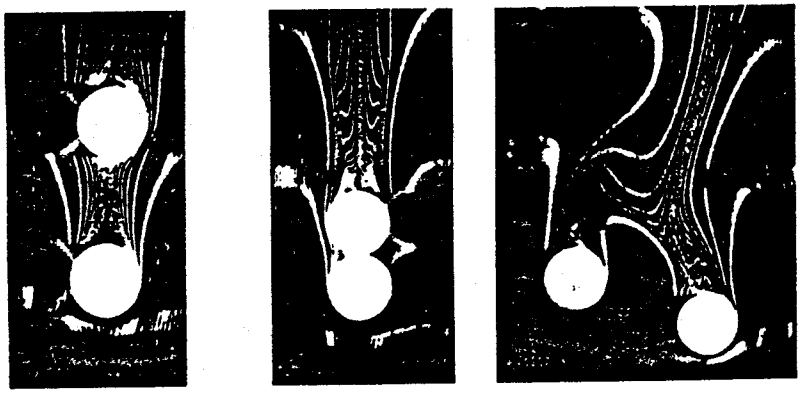

Figure 10.4.2 Interaction of two Delrin spheres 11.113 mm diameter at Re=8.5, showing drafting, kissing and tumbling.

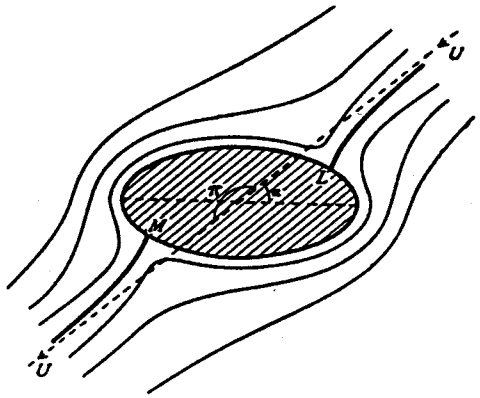

Figure 10.4.3 Potential flow solution for uniform flow past a slender body. The high pressure at the points of stagnation give rise to a couple causing the body to turn broadside-on. In real flows this mechanism operates only on the front side, with a wake on the back.

The robust stability of the cross stream alignments are particularly dramatic in a two-dimensional bed of a single line of particles (see figures 10.4.8 and 10.5.1). It is perhaps a subtle feature of nature that the same hydrodynamic forces which cause long bodies to float broadside-on endow beds of tumbling spheres with an anisotropic structure of horizontal arrays which may lend itself to study in a one-dimensional approximation.

It must be noted that the drafting of spheres is a rearrangement mechanism which sucks spheres together, an effect of an entirely different natutre than the Brownian type of motions which cause spheres to diffuse into empty places by the mechanism which is invoked to explain the stabilizing action of the particle phase pressure (Batchelor 1988). Wakes lead to aggregation rather than dispersion. The photographs shown in figures 10.4.4 to 10.4.9 show how aggregates may form and collapse under the action of wakes. The formation and collapse of aggregates appears to be closely related to the propogation of voidage waves in a manner to be inferred by comparing figures 10.4.4 with 10.4.6 and 10.4.5 with 10.4.8. In the typical case voidage shock waves propogated by a mechanism in which particles fall out of the aggregate at the roof of the void and collect at the top of the aggregate at the floor of the void as in our figures 10.4.6 and 10.4.8, and in figure 10 of Fortes, et al. (1987). This type of shockwave of voidage is called slugging in three-dimensional fluidized beds and is well-known.

The reader should wonder how in the world the aggregates at the top of the beds shown in figures 10.4.4, 10.4.5 and 10.4.7 ever formed. They are stationary aggregates of close-packed spheres, porous media, held together

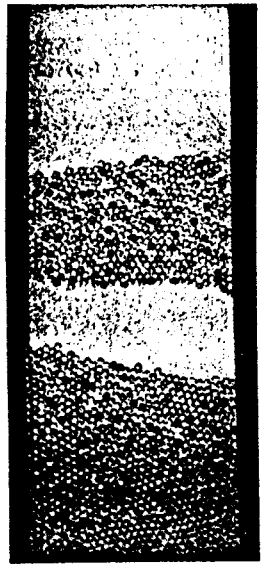

Figure 10.4.4 A stationary void and stationary aggre-gates of 0.231 diameter glass beads in a 6 inch bed. Re=1400 is based on the sphere diameter and fluidi-zation velocity. This is a stationary voidage shock, a two-dimensional "slug." The bed is slightly inclined from the vertical (20°) and wall friction helps to stabilize the shock wave.

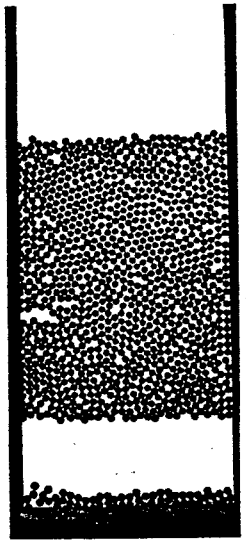

Figure 10.4.5 A stationary void and stationary aggre-gates of a $\frac{1}{4}$ inch plastic spheres in a 6 inch bed, Re=380.

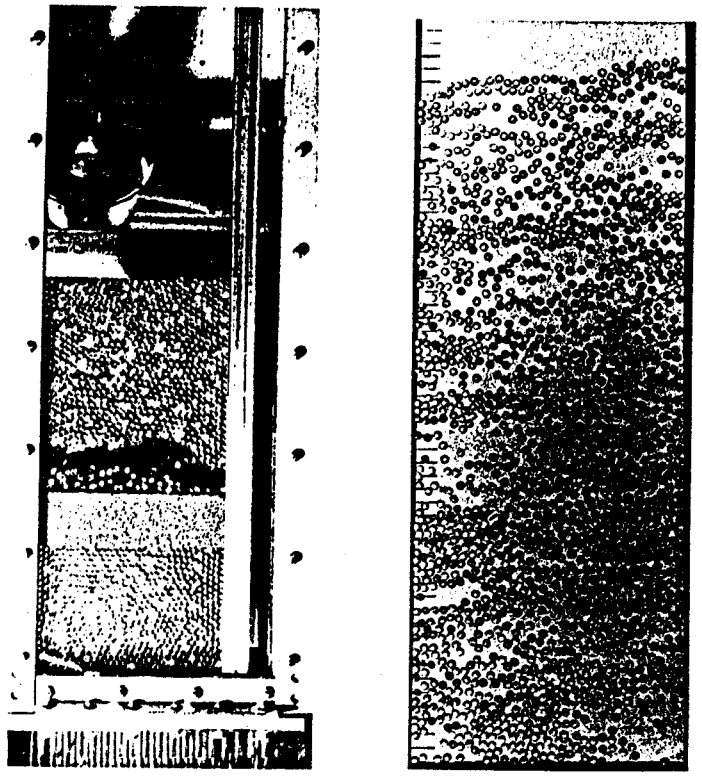

(a) (b)

Figure 10.4.6 Propagation of voidage waves in beds of 0.231 in glass beads in water. (a) A shock wave of voidage propagates by particle release from aggregate at the roof of the void. (b) A bed has expanded but close-packed clusters are still in evidence. The clusters appear to be held together by wake forces. The spheres are either in clusters, in cross stream arrays or they are drafting, kissing and tumbling.

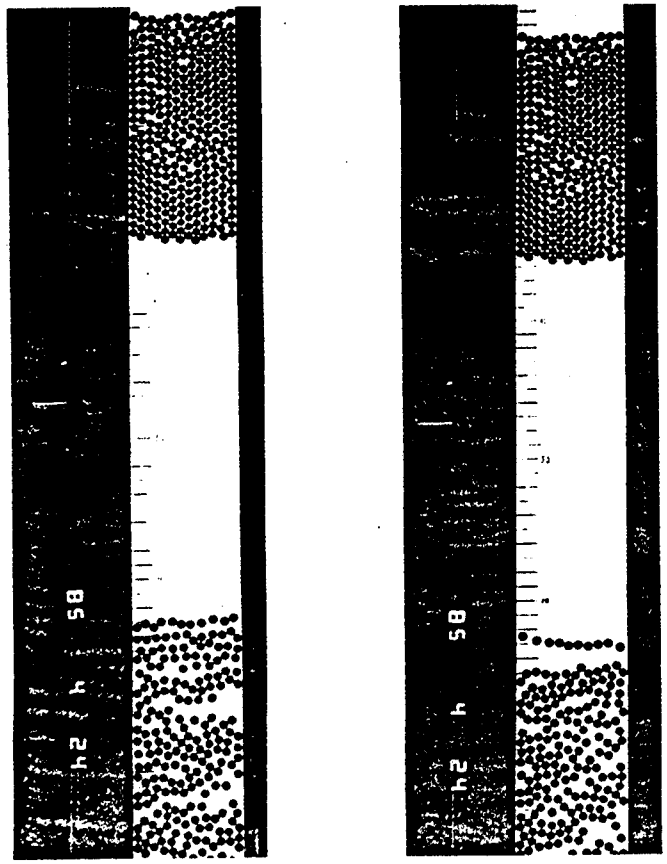

(a) (b)

Figure 10.4.7 A stationary shock wave, closed-packed, $\frac{1}{4}$ inch diameter plastic spheres at the top of the void and propagating "one dimensional" voidage waves at the bottom of a 3 inch bed, Re=390. There is nothing to restrain the aggregated beads at their top or bottom, other than hydrodynamic forces. Earlier, the aggregate formed by sucking spheres into the bottom row of the packed bed.

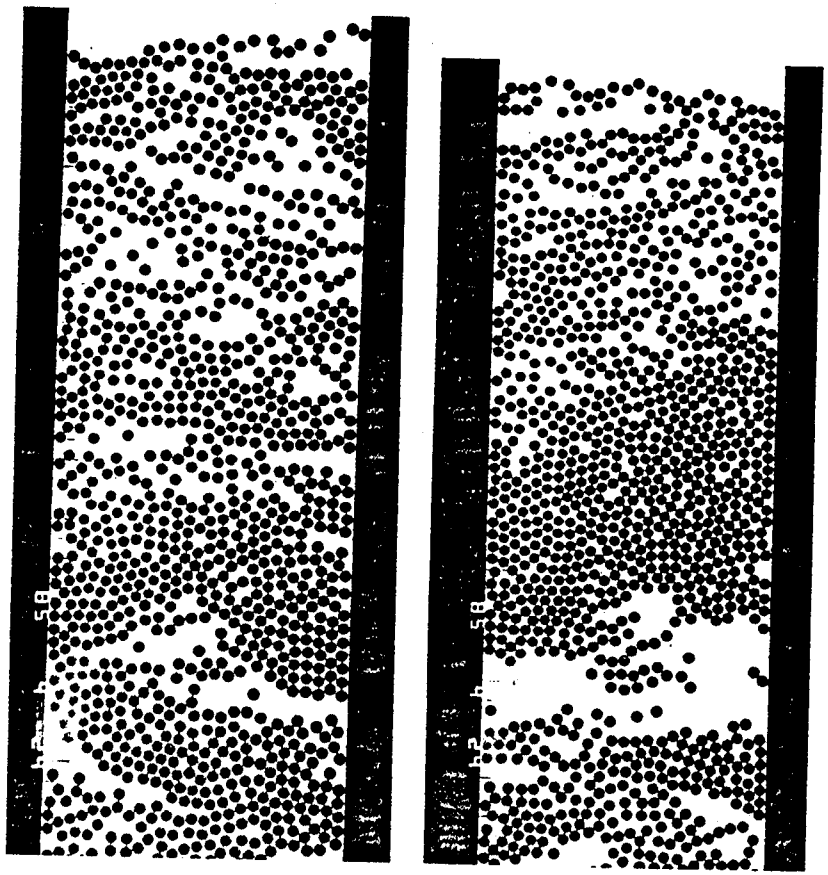

(a) (b)

Figure 10.4.8 Fully fluidized bed of $\frac{1}{4}$ inch plastic spheres in a six inch bed, Re= 370. It appears as if there are clusters of spheres which are not individually fluidized. We think that these clusters are held together by mutual interactions of wakes. The spheres are either in clusters, in cross stream arrays or are drafting, kissing and tumbling.

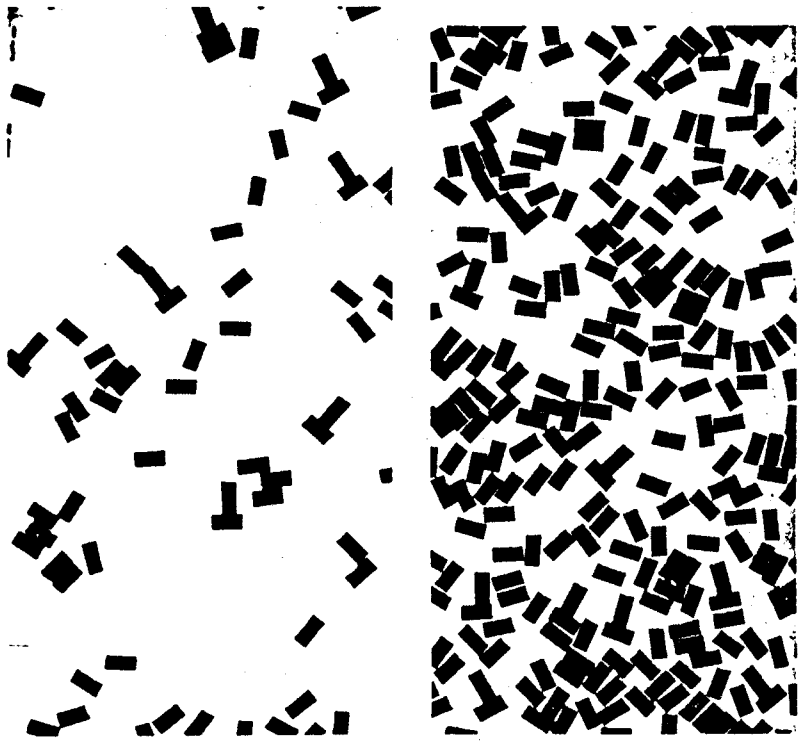

Figure 10.4.9 Fluidization of round cylinders with flat ends, l/D≈2. Individual cylinders rock violently from vortices shed at the sharp corner at a Reynolds number $0(10^3)$. They oscillate around the horizontal. Wake interactions are evident in the piles of cylinders which contact along their long sides, and in the characteristic inverted T in which the top cylinder stands end on in the wake of the bottom. The formations are examples of wake architectures. Most of the cylinders are glued by wakes in small clusters dispersed over the bed. We may entertain the idea that the clusters defined by range of influence of the wakes in a given architecture are dispersed in the flow, rather than the individual particles.

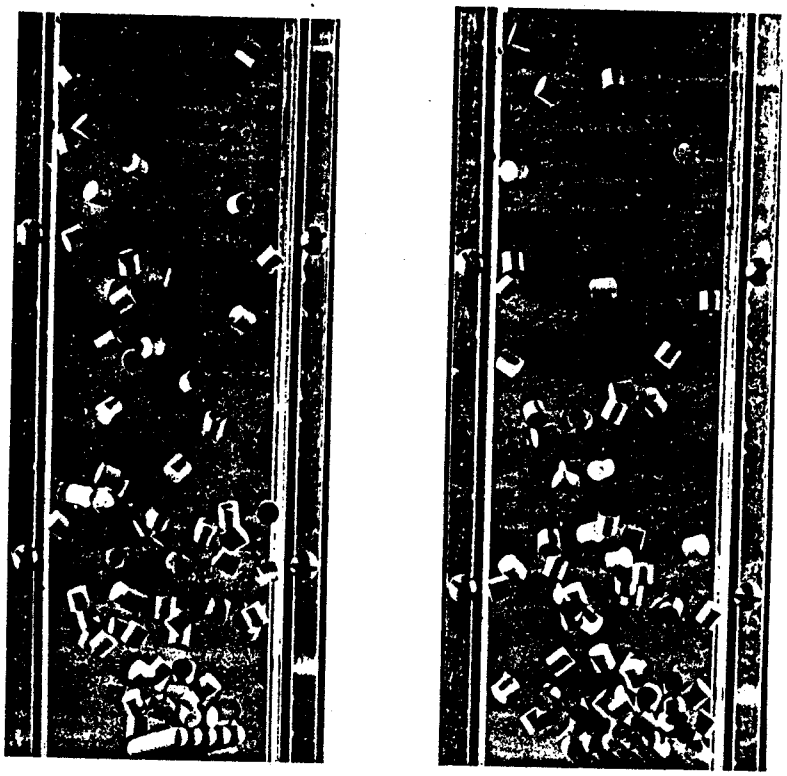

Figure 10.4.10 Short cylinders are sucked into the wake of a raft made by glueing five long cylinders. The raft is fluidized in water in a three-dimensional bed and the drag of short cylinders and the raft is about the same. The raft always floats broadside on and the violent fluctuations around the mean due to vortex shedding are suppressed by the short cylinder.

by hydrodynamic forces only, we think by the wakes behind each and every sphere in the array. We have seen how particles drift into these aggregates when they are close to the roof of the void and other conditions which we have not identified are satisfied. They are pulled in by pressure forces which we think are generated in the wakes behind the aggregated spheres, clearly a three-dimensional effect for close-packed spheres in a two-dimensional bed. This formation of aggregates is exactly the inverse of mechanism which causes propogation of voids because the particles are sucked into, rather than released from, the packed aggregate at the roof of the void. The whole matter could stand more study.

It is well-known, but I think less well known than it ought to be, that the average orientation of a long body moving relative to a stream is robustly stable when the long side is across the stream.

> Thus a ship has to be kept on course by the helmsman, an elongated airship requires similar attention. A sailing ship will not sail permanently before the wind with the helm lashed, but tends to set itself at right angles to the wind. A body sinking in liquid tends to sink with its longest dimension horizontal (Milne-Thompson 1960).

The tendency for long bodies to float broadside on in a two-dimensional flow is the same as the tendency of flat or broad body to float with its broad side facing the flow in a three-dimensional setting. This, together with the well-known power of wakes behind blunt bodies is exhibited in figure 10.4.10 where we show small cylinders bombarding a fluidized raft floating broadside on. The raft was made by glueing five long cylinders together and when fluidized without the short cylinders, it rocked with a frequency which we suppose to be associated with vortex shedding around an equilibrium position perpendicular to the stream. We matched the drag on the raft with the drag on a small cylinder of length/diameter = 0.25in./0.0255in. and fluidized many such cylinders with the raft. The cylinders are sucked into the wake of the raft like debris behind a fast-moving truck. The composite body, raft plus entrained cylinders, is very stable; the oscillations are greatly suppressed.

10.5 STABLE WAKE ARCHITECTURES

Many stable configurations of spherical and long particles have been found in our experiments in two-dimensional beds. Some of them were described in the papers by Fortes, et al. (1987) and Joseph, et al. (1987) and some will be described in a forthcoming paper by Fortes and Joseph (1991). These stable configurations appear to be held in place by wake forces and turning couples in a manner of whose details have yet to be determined. The stable configurations found so far are

(1) Stable horizontal line of spheres (figure 10.5.1)
(2) Stable arch of aluminim spheres (figure 10.5.2)
(3) Nested wake of two spheres (figure 10.5.3)
(4) Nested wake of three spheres (figure 10.5.3)
(5) Nested wake of four spheres (figure 10.5.3)
(6) Stable doublets of long particles (figure 10.5.4)
(7) Stable triplets of long particles (figure 10.5.4)
(8) Stable quadruplets of long particles (figure 10.5.4)

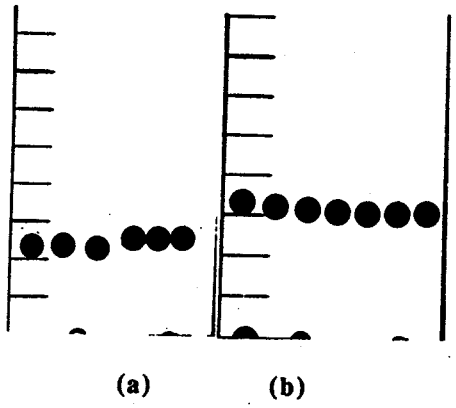

Figure 10.5.1 Long bodies float broadside on and spheres line up broadside on. (a) Three cemented spheres on the right are robustly stable when their line of centers is perpendicular to the stream. Three spheres on the left are not cemented. They line up broad-side on because otherwise they would interact in the wakes of other pairs. (b) A line of seven individual spheres fluidized with their line of centers perpendicular to the stream.

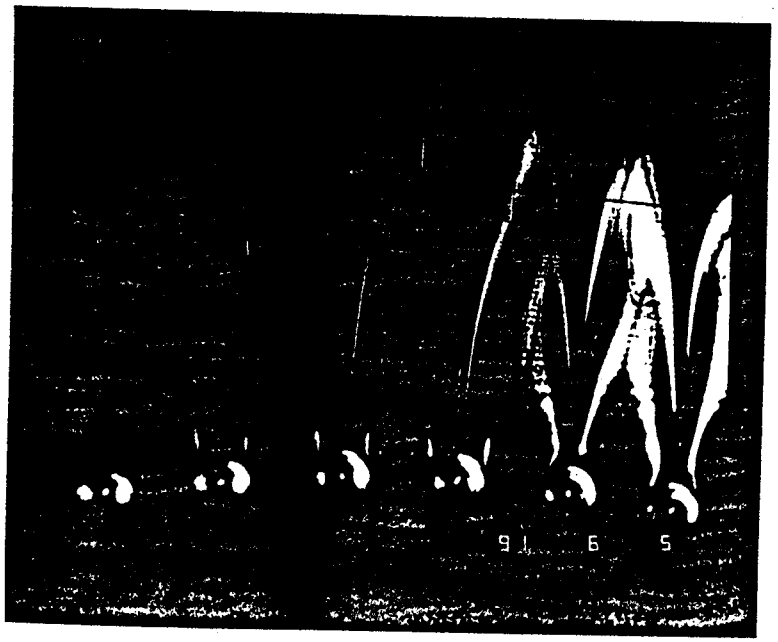

Figure 10.5.2 Stable arch of aluminum spheres.

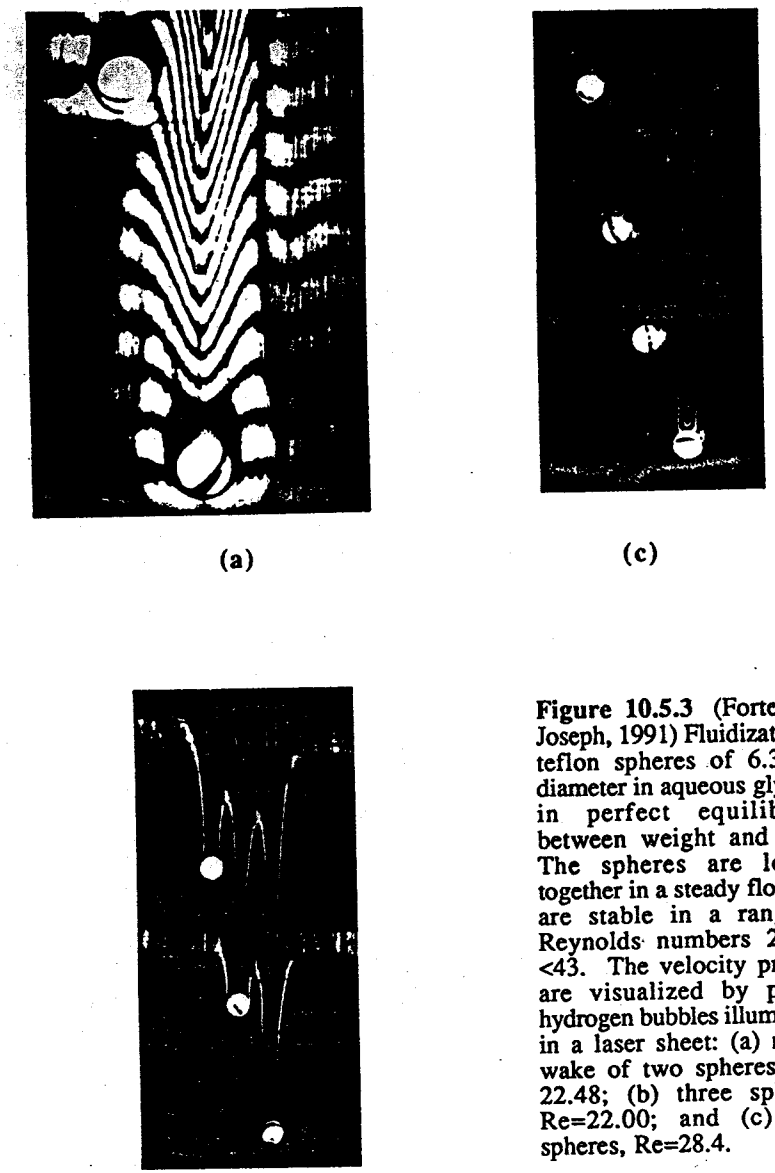

Figure 10.5.3 (Fortes and Joseph, 1991) Fluidization of teflon spheres of 6.3 mm diameter in aqueous glycerin in perfect equilibrium between weight and drag. The spheres are locked together in a steady flow and are stable in a range of Reynolds numbers $22<Re<43$. The velocity profiles are visualized by pulsed hydrogen bubbles illuminated in a laser sheet: (a) nested wake of two spheres, Re= 22.48; (b) three spheres, Re=22.00; and (c) four spheres, Re=28.4.

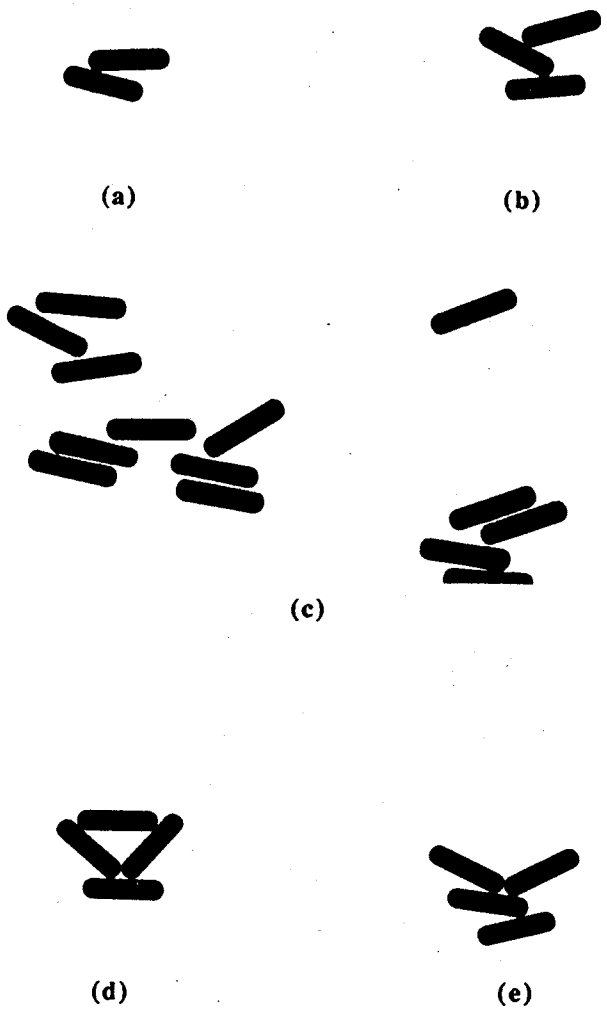

Figure 10.5.4 Stable doublets, triplets and quadruplets. Long bodies float broadside on. They generate strong wakes. If several long bodies are present, they interact to form stable wake architecture: (a) stable doublet, (b) stable triplet of the first kind, (c) stable triplets of the first and second kinds form on the left, (d) stable quadruplet, and (e) stable quadruplet of the second kind.

We are going to confine our explanations of the remarkable stability of these configurations to captions on the figures. It is our belief that a good theoretical understanding of stable wake architectures can be best achieved by comparing experiments with direct numerical simulation of the Navier-Stokes equation and the particles equation of motion. The first paper to move in this direction, by Singh, Caussignac, Fortes, Joseph and Lundgren (1989) who tested the stability of such a single line of particles (as in figure 10.5.1a) in a direct, but strictly two-dimensional simulation of the Navier-Stokes equations for steady flow across circular cylinders Re<100. They perturbed the periodically spaced horizontal line of circular cross sections of cylinders all equally spaced in various ways and computed the steady flow and the hydrodynamic forces on the cylinder to see if the forces would tend to restore stability. They found that the two-dimensional array was stable to small disturbances with greater stability for high Reynolds numbers. A further step was taken recently by Hu, Crochet and Joseph (1991) who computed the trajectories of "spheres" dropped from rest in a channel. They found that a single cylinder sedimenting in a channel at small Reynolds numbers will drift to the center of the channel. The channel center appears to be an equilibrium position at Reynolds numbers below the critical one for vortex shedding. At higher Reynolds numbers the cylinder drifts off the center of the channel. It rotates due to uneven shear and oscillates due to vortex shedding.

The numerical simulation for two sedimenting cylinders gave rise to the kind of drafting, kissing and tumbling which is observed in the sedimentation (and in the fluidization) of two spheres. However, unlike the spheres the cylinders do not actually touch and appear to repel each other at a distance at large Reynolds numbers apparently due to lubrication forces or to a failure of the numerical scheme for touching cylinders at small Reynolds numbers.

A detailed comparison of the two-dimensional computation with the two-dimensional motion of sedimenting spheres has yet to be made. There is a huge body of information which can be exracted from the two-dimensional simulations but eventually a full three-dimensional will be needed. The two-dimensional bed is an excellent laboratory for comparing computations with experiments because everything can be seen.

10.6 SUMMARY

We have considered three effects which are neglected in conventional theories of fluidized suspensions: finite size effects, wakes and turning couples on long bodies and on spherical bodies in momentary contact.

We developed a three variable, one-dimensional, one-phase theory to account for the finite size of particles. The theory uses the Foscolo-Gibilaro force law except that the force that the fluid exerts on the solid is assumed to depend on the fractional area rather than the volume fraction of solids and the gradient of the volume fraction which expresses the particle phase pressure is put to zero. The area and volume fraction are related by a simple geometrical construction in the case of fluidization of a monodisperse suspension of spheres of radius R, taking into account the fact that the portion of the plane at Z blocked by particles is determined also by spheres whose centers are not at Z. Our one-dimensional theory then has three unknowns, the volume fraction, the area fraction and particle velocity, rather that two. These equations admit uniform fluidization as a solution which is Hadamard unstable in the two-variable theory but simply unstable in the three-variable theory, with a distinguished set of marginally stable modes belonging to a countable set of blocked wave numbers generated by the relation between the volume and area fraction. The blockage function regularizes the ill-posed problem and generates a structured dynamical response with a set of discrete stationary marginal modes. The finite size, three-variable theory reduces to the conventional two-variable theory as the particle radius R tends to zero, but not uniformly. The limiting problem is never ill-posed, the maximum growth rate Σ_m is at an approximate wave number of 1.3/R, and is therefore bounded for any finite R no matter how small. The initial value problem for our three-variable, one-dimensional theory is solved by numerical methods for periodic boundary and different initial conditions. Solutions are bounded with nearly stationary power when Σ_m is small, and no such solutions exist when Σ_m is large. The power spectrum of bounded solutions contains low power for the blocked wave numbers and is in astonishing agreement with the values of the power spectrum measured in the experiments of Singh and Joseph (1991 a, b) with fluidized spheres constrained to move in two dimensions (see figure 3.3).

The nonlinear effects, which are neglected in conventional treatments of fluidized suspensions, are associated with wakes and the moment distributions of hydrodynamic forces on long bodies (and spheres in near proximity), which tend to turn the bodies so that the long side (or line of centers) is perpendicular to the stream. These mechanisms are active in the balance that determines the main features of fluidization at all but the smallest Reynolds numbers and they are of practical importance. Nonlinear fluidization of spheres is dominated by mechanisms associated with drafting, kissing and tumbling which are illustrated in figures 4.1 and 4.2. The drafting of spheres is a wake effect which sucks particles together; exactly opposite to the effects of hydrodynamic dispersion in which fluctuations drive particles apart. Many robust effects of aggregation can be explained by wake effects which are neglected in conventional theories. The tumbling of spheres into positions with lines of center perpendicular to the stream, gives an anisotropic structure to the bed in which cross-stream alignments are favored. The nonlinear mechanisms underway in the fluidization when there are only a few particles, are accessible to rigorous treatment by numerical simulations using the Navier-Stokes equations and the particles equations of motion.

ACKNOWLEDGEMENTS

This work was supported by the National Science Foundation and the Department of Energy. Numerical results were obtained under grants from the Minnesota Super Computer Institute and AHPCRC.

REFERENCES

Batchelor, G.K., A new theory of the instability of a uniform fluidized bed. *J. Fluid Mech.*, 193, pp. 75-110 (1988).

Fortes, A., D.D. Joseph, and T. Lundgren, Nonlinear mechanics of fluidization of beds of spherical particles. *J. Fluid Mech.*, 177, pp. 467-483 (1987).

Fortes, A., and D.D. Joseph, Wake architectures in two-dimensional fluidization of spheres. *AHPCRC* preprint 91-68 (1991).

Foscolo, P.V., and L.G. Gibilaro, A fully predictive criterion for transition between particulate and aggregate fluidization. *Chem. Eng. Sci.*, **39**, pp. 1667-1674 (1984).

Foscolo, P.V., and L.G. Gibilaro, Fluid dynamic stability of fluidized suspensions. The particle bed model. *Chem. Eng. Sci.*, **42**, pp. 1489-1500 (1987).

Hu, H., M.J. Crochet, and D.D. Joseph, Direct simulation of fluid particle motion. AHRCRC Report 91-45. Submitted to *Theor. Computat. Fluid Dynamics* (1991).

Happel, J., and R. Pfeffer, The motion of two spheres following each other in a viscous fluid. *A. I. Ch. E. Journal*, **6,1**, pp. 129-133 (1960).

Jackson, R., The mechanics of fluidized beds: Part I: The stability of the state of uniform fluidization. *Trans. Instn. Chem. Engrs*, **41**, pp. 13-21 (1963).

Jones, A.V., and A. Prosperetti, On the suitability of first-order differential models for two-phase flow prediction. *Int. J. Multiphase Flow*, **11**, pp. 133-148 (1985).

Joseph, D.D., A. Fortes, T. Lundgren, and P. Singh, Nonlinear mechanics of fluidization of beds of spheres, cylinders and disks in water. Advances in multiphase flow and related problems. Ed., G. Papanicolau, *SIAM*, pp. 101-122 (1987).

Joseph, D.D., Generalization of Foscolo-Gibilaro analysis of dynamic waves. *Chem. Eng. Sci.*, **45**, pp. 411-414 (1990).

Joseph, D.D., and T.S. Lundgren, Ensemble averaged and mixture theory equations for incompressible fluid-particle suspensions. *Int. J. Multiphase Flow*, **16**, pp. 35-42 (1990).

Milne-Thompson, L.M., Theoretical hydrodynamics. *4th Ed. Macmillan*, pp. 530 (1960).

Prosperetti, A., and A.V. Jones, The linear stability of general two-phase flows models-II. *Int. J. Multiphase Flow*, **13**, pp. 161-171 (1987).

Prosperetti, A., J.V. Satrape, Two phase flows in fluidized beds, sedimentation and granular flows. IMA volumes in Mathematics and its Applications 26, *Springer-Verlag*, pp. 98-117 (1989).

Richardson, J.F., and W.N. Zaki, Sedimentation and fluidization: Part I. *Trans. Instn. Chem. Engrs*, **32**, pp. 35-53 (1954).

Singh, P., P. Caussignac, A. Fortes, D.D. Joseph, and T. Lundgren, Stability of periodic arrays of cylinders across the stream by direct simulation. *J. Fluid Mech.*, **205**, pp. 553-571 (1989).

Singh P., and D.D. Joseph, One-dimensional, particle bed models of fluidized suspensions, two phase flows in fluidized beds, sedimentation and granular flows. IMA volumes in Mathematics and its Applications 26, *Springer-Verlag*, pp. 130-149 (1990).

Singh, P., and D.D., Joseph, Dynamics of fluidized suspensions of finite size. AHRCRC Report 91-60. Submitted to *J. Fluid Mech.* (as a revision of the 1989 paper "Chaos and structure in two-dimensional beds of spheres fluidized by water") (1991a).

Singh, P., and D.D. Joseph, Finite size effects in fluidized beds in liquid-solid flows. FED 118, Eds. M.C. Roco and T. Mayasuma, *American Society of Mech. Engrs.*, pp. 77-86 (1991b).

Volpicelli, G., L. Massimilla, and F.A. Zenz, Non-homogeneties in solid-liquid fluidization. *Chem. Eng. Symp. Series*, **67**, pp. 62, 42-50 (1966).